Available online at www.sciencedirect.com
ScienceDirect
Journal of Nuclear Materials 363–365 (2007) 12–23
journal of nuclear materials
www.elsevier.com/locate/jnucmat

Key plasma wall interaction issues towards steady state operation

E. Tsitrone *

Association EURATOM–CEA, CEA/DSM/DRFC CEA Cadarache, 13108 Saint Paul Lez Durance cedex, France

Abstract

With the ITER construction approaching, fusion devices have started to tackle the technological and physical challenges associated with steady state operation. Significant progress has been achieved with pulses longer than 400 s and coupled energy larger than 1 GJ. This shed a new light on plasma wall interactions (PWI), occurring over long time scales. The main PWI limitations for long pulses are localized heat loads associated with fast particles losses, and density control linked to outgassing from heated plasma facing components (PFCs). In long pulses, particle recovery after shot is independent of the retained fuel, leading to a significant wall inventory build up in contrast with short pulses. Different retention mechanisms (codeposition, implantation, bulk diffusion) have been identified as dominant, depending on the plasma and PFCs characteristics. However, the above results have been obtained with carbon PFCs, leaving effects related to the material mix foreseen for ITER as an open issue.

PACS: 52.40.Hf; 52.55.Fa; 52.55.Rk

Keywords: Steady state; Density control; Active cooling; Wall pumping; Deuterium inventory

1. Introduction

Extending reliably plasma fusion regimes towards a steady state scenario, going from peak to sustained performance, is a major issue for next step devices, both from the physics and technology point of view [1]. Today, addressing this issue is becoming a worldwide effort, as various devices started to tackle this challenge. Some of them are especially designed for long pulse studies, and are in particular equipped with superconducting coils (Tore Supra (TS), HT7, LHD, Triam-1M). So are most new devices now under construction (EAST, KSTAR, SST-1, JT60-SA, W7X). Others have recently been upgraded to extend their pulse duration (JT60U, JET, DIIID, AUG) despite copper coils. This paper summarizes progress obtained in recent years towards steady state operation, with a focus on plasma wall interactions (PWI) related issues. Section 2 briefly reviews physical and technical constraints associated with long pulse operation. Section 3 presents the recent achievements obtained in present day devices, and their relevance to PWI issues for ITER. Section 4 lists the main PWI limitations to long pulse operation, and how to

* Tel.: +33 442 254962; fax: +33 442 254990.
E-mail address: emmanuelle.tsitrone@cea.fr

0022-3115/$ - see front matter
doi:10.1016/j.jnucmat.2006.12.057

overcome them. Section 5 is devoted to fuel retention, a critical issue for ITER on which long pulse operation has allowed to gain insight. Summary is presented in Section 6, where open issues are mentioned, as well as future prospects for steady state operation.

2. Physical and technical constraints for steady state

From the core physics point of view, 'steady state' means a discharge duration longer than several plasma current diffusion times τ_R (10^{-1} to seconds depending on the device) to reach constant loop voltage conditions. Discharges from 10 s (DIIID) up to minutes (Tore Supra) or hours (TRIAM-1M) are called 'long pulses'. However, PWI characteristic time scales often exceed τ_R, going from 10s of seconds (thermal equilibrium of plasma facing components (PFCs)) to 100s of seconds (wall saturation) up to 10^6 s (PFC lifetime). This paper will concentrate on discharges relevant for PWI, typically longer than 10 s.

Running steady state discharges requires a strong integration between technology and physics:

- to sustain the magnetic configuration, with superconductive coils and non inductive current drive (except for stellarators or heliotrons);
- to inject and exhaust power, with long pulse capacity heating systems and actively cooled PFCs;
- to inject and exhaust particles, with long pulse capacity fuelling systems and active pumping;
- to control the discharge with real time feedback control schemes.

The main constraints on the scenario come from the available power for non inductive current drive, determining the plasma current/density achievable for a given pulse duration. Moreover, regimes close to zero loop voltage are often prone to MHD instabilities, and require careful adjustment of the current profile evolution. Finally, the scenario must be compatible with power coupling and minimize localized heat loads (see Section 4), limiting the range of operational density and plasma current. In addition, devices not equipped with superconductive coils have access to restricted magnetic configurations (reduced magnetic field, X point height and triangularity), and those not actively cooled must lower the additional power. Therefore, present day experiments are often restricted to low density/low plasma current discharges when running long pulses, while next step steady state devices are expected to operate at high density/high current for better fusion performance.

3. Recent achievements in long pulse operation

Despite those limitations, major progress in long pulse operation has been obtained in recent years. The main achievements are presented on Fig. 1. Three categories of devices can be distinguished:

- Conventional coils, no active cooling (JET, JT60U, DIIID): those devices aim at extending the duration of high performance regimes, but have restricted pulse duration (typically less than a minute). Remarkable progress has been achieved, such as high β_N discharges performed in JT60U (~20 s, 10 MW, 200 MJ [2]) and DIIID (~12 s, 4 MW, 40 MJ [3]) as well as sustained ITB regimes in JET (20 s, 18 MW, 326 MJ [4]). Long L mode discharges have also been produced in JET (~60 s, 4 MW, 240 MJ [4]) as well as long H mode discharges in JT60U (65 s flat top, 30 s H mode at 10 MW, ~300 MJ [2]), in particular for particle balance studies.
- Superconductive coils, no active cooling (LHD, HT7, TRIAM-1M): those devices can access long discharges but are restricted in power (typically

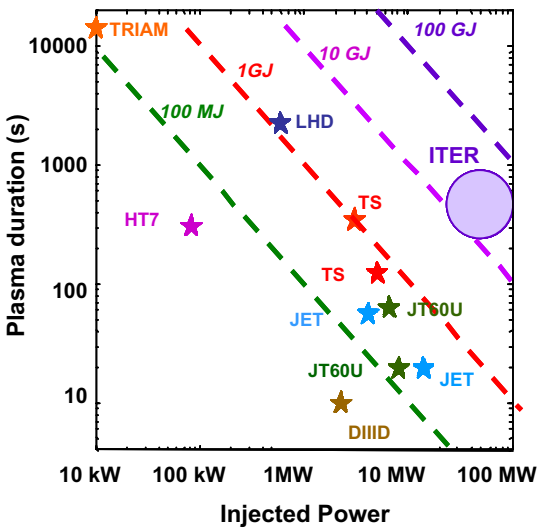

Fig. 1. Best performances obtained in long pulse operation in terms of plasma duration as a function of injected power for present day devices: JET, JT60U, DIIID, HT7, LHD, TRIAM-1M, TS.

Table 1
Relevance of present day long pulse experiments to ITER PWI issues [10]

	AUG	JET	JT60U	LHD	HT7	TRIAM	TS	ITER [10]
Configuration	Ax div	Ax div	Ax div	Isl div	lim	lim	lim	Limiter / Ax divertor
PFC material	C / W	C / Be evap	C	C	C	Mo	C	C / W / Be
Particle flux > 10^{22} D/m^2/s	yes	yes	yes	no (He)	no	no	yes	10^{23} D-T /m^2/s
1 < Te < 10 eV(semi detach)	yes	yes	yes	yes	yes	yes	no	1-10 eV on targets
Pulse > 1 mn	no	~	~	yes	yes	yes	yes	400s
Power flux > 1 MW/m^2	yes	yes	yes	no	no	no	yes	10 MW/m^2 (+ transient)
Active cooling	no	no	no	no	no	no	yes	yes

Dark grey zones show significant deviation from ITER parameters.

less than 1 MW). LHD recently broke the injected energy record (1900 s, 700 kW, 1.3 GJ [5]; 3300 s, 500 kW, 1.6 GJ [23]). HT7 significantly extended its pulse duration (300 s, 100 kW, 30 MJ [6,7]), while TRIAM-1M performed ultra long discharge at low power (5h16, 10 kW, ~200 MJ [8]).

- Superconductive coils, active cooling (TS, future projects listed in Table 2): those devices can access long pulse with significant coupled power, and most machines now under construction belong to this category, including ITER. TS was able to couple more than 1 GJ of energy to the plasma (378 s, 3 MW, 1.1 GJ [9]), and has recently extended its long pulse database to higher density/power regimes (80 s, 7 MW, ~500 MJ [30]).

The relevance of these experiments to PWI issues in ITER is presented in Table 1, with criteria such as magnetic configuration, PFC material, pulse duration, active cooling of PFCs. Representative plasma conditions in terms of particle and power fluxes, plasma temperature have been added. Dark grey zones in the table indicate significant deviation from ITER parameters [10]. From looking at Table 1, two issues are clearly poorly addressed. The first one is the PFC materials: most today long pulse experiments rely on carbon PFCs, and this paper will therefore only present carbon related results, although mixed material effects are a crucial point to explore for ITER [11]. The second one is active cooling. Running long pulses on non actively cooled PFCs, as well as with a non zero loop voltage, should not strictly be considered as 'steady state'. In particular, a rising temperature T_{surf} for PFCs all along the discharge has significant implications on PWI, specifically on material erosion and fuel retention. Indeed, carbon PFCs (as mostly used in present day devices) can enter different erosion regimes during the discharge: physical sputtering at low T_{surf} (<400 °C), chemical erosion at intermediate T_{surf}, and thermal sublimation for high $T_{surf} > 2000$ °C. This impacts the carbon source, and consequently codeposition of the fuel with the eroded material. Moreover, the maximum concentration C_{Dmax} before reaching saturation for implantation of deuterium (D) in carbon (C) strongly decreases with increasing T_{surf} (see Fig. 10 in [12]). Therefore, net wall pumping can turn into net wall outgassing as T_{surf} increases during the discharge. This has to be kept in mind when interpreting experiments in non actively cooled devices. Finally, it should be noted that ITER will also be a long pulse experiment in limiter configuration during the plasma ramp up phase (~30 s) [13], which makes contribution from limiter machines also valuable (therefore light grey in Table 1). LHD, with its island divertor, is in a relevant plasma regime although in a quite different geometry and so also appears in light grey.

4. PWI limitations for long pulse operation

The main PWI limitations for long pulse operation concern power exhaust, density control, and

plasma contamination by impurities. These issues are closely linked, as overheating of PFCs often results in outgassing, yielding uncontrolled density rise as well as impurity emission.

4.1. Power exhaust

As far as power exhaust is concerned, improving PFCs allows to extend the discharge duration by providing an easier density control: from 160 to 300 s [6] in HT7 with new top/bottom toroidal limiters, and guard limiters for lower hybrid (LH) couplers [14,15]; from 3 h to 5 h in TRIAM-1M by inserting a movable cooled limiter [8,16]. In LHD, improved conductivity graphite sheets were inserted between the plasma facing materials and the heat sink. In addition, plasma sweeping was performed in order to divert the power flux from upper to lower divertor plates every 100 s, thus limiting the PFCs temperature increase. This allowed to extend the pulse duration from 160 s to 1800 s [5,17]. However, for significant heat loads (>1 MW/m^2), only active cooling becomes relevant to keep PFCs temperature in a reasonable range for long pulse operation. With its new generation of actively cooled PFCs installed during the CIEL upgrade [18], TS extended its pulse duration from 2 to 6 mn [9] (the present limitation being the long pulse capacity of the heating systems, not power handling).

However, the main issue for power exhaust in long pulses comes from fast particle losses generated when coupling power to the plasma (fast ions from NBI or ICRH, electrons accelerated by LH...): they generally carry a small fraction of the coupled power, but impact very locally on the PFCs, giving rise to high localized heat loads (>1 MW/m^2). This effect is benign on short pulses, but not tolerable on long pulses [19]. In order to overcome this problem, ferritic inserts have been installed in HT7 and JT60U to reduce the ripple and the associated particle losses [7], and specific protection tiles were added in TS [20], decreasing the overall iron (Fe) level in the discharge [34]. Identifying the physical processes involved (RF sheaths, ripple losses ...) is underway [21–24] in order to optimize the plasma scenario for avoiding hot spots on PFCs, and developing control schemes.

4.2. Density control

However, the most serious limitation encountered on all machines aiming at long pulse operation is density control [25–27]. After a given duration, depending on the coupled power and the plasma density, an uncontrolled density rise often takes place despite cutting plasma fuelling and terminates the discharge (see Fig. 2). Plasma performance is also affected by the loss of density and recycling control, with a progressive confinement degradation as the density rises in JT60U long H mode discharges [28]. This density rise seems to be associated with outgassing from heated components, rather than wall saturation by deuterium. Indeed, it was also observed in helium discharges in LHD, and correlated with toroidally localized Hα emission from components heated by local ICRF losses [17,29]. Moreover, detailed analysis in TS before the CIEL upgrade [25] lead to the conclusion that the plasma density increase was due to water outgassing, probably coming from components located far away from the plasma (such as ports) heated by

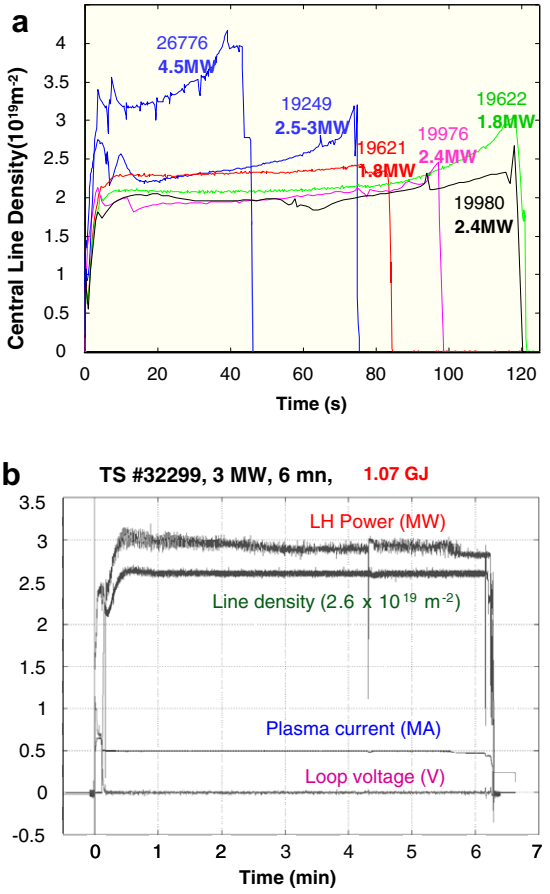

Fig. 2. Uncontrolled density rise observed in TS before the CIEL upgrade [25] (a) and density control demonstrated up to 6 mn in TS after the CIEL upgrade [30] (b).

radiated flux, and not from the actively cooled main PFCs. Although the temperature increase on these components was estimated to be small ($\Delta T =$ 20 °C), it was enough to generate significant outgassing as these parts of the machine were not properly conditioned. Therefore, special attention was taken during the CIEL upgrade to efficiently screen the vacuum vessel from radiated flux, and to ensure extensive baking and cooling of components, including ports. In these conditions, uncontrolled outgassing is not observed anymore, and density control was demonstrated up to 6 mn (see Fig. 2) [9,30]. In JT60U, improving divertor pumping by optimizing the plasma position was demonstrated to efficiently reduce the density increase rate [2,31]. However, the wall inventory is estimated to be a much larger particle reservoir than the plasma content, and very sensitive to T_{surf} variations. Therefore, it might seem difficult to control the plasma density by active pumping only if significant outgassing takes place, as pumping systems are designed to exhaust moderate particle fluxes (~fuelling rates, a few % only of the recycling fluxes). In order to ensure density control for long pulse operation, besides active pumping, special care should be taken for active cooling/baking of the totality of the vessel, including remote parts.

4.3. Impurity contamination

As far as impurities are concerned, boronisation is often used before running long pulses to reduce the overall level of oxygen (O) and metallic impurities [32,33]. The current drive efficiency is improved when the impurity content of the plasma is reduced, allowing for better performance, although the effect seems to be small on machines where Z_{eff} is dominated by carbon like TS [34]. Other conditioning methods, like He GDC or RF cleaning, are also used to operate with a good wall pumping capacity and avoid density control issues [6]. However, it should be kept in mind that conditioning procedures used on present day machines are not expected to remain efficient after the start up phase for next step devices like ITER, due to the increased pulse length and associated high particle fluence.

Although not specific to long discharges, impurities bursts can impede steady state operation. They are often correlated with hot spots from impacting fast particles or arcing on the RF heating systems [35]. This is recognized as being one of the present limitations for long pulse operation in LHD [17]. In TS, real time IR control was implemented to detect arcs and hot spots on the RF couplers [36].

In LHD, impurity accumulation is observed in plasma conditions coherent with the neoclassical transport theory [37], therefore not specific to long discharges. Control of the impurity accumulation by an externally induced magnetic island in the plasma edge was demonstrated.

However, some impurity behaviours are more specific to long pulses. In TS, although Z_{eff}, dominated by C, is constant during the discharge, a slow rise of the Fe and O levels is sometimes observed [34], which could be linked to a progressive change in the wall composition, as impurities are being eroded and transported from remote locations to locations from where they can enter the main plasma. In TRIAM-1M, regular ultra low frequency oscillations with progressive Mo accumulation and decay are observed [8], on time scales of ~100 s, eventually terminating the discharge.

5. Insight on fuel retention from long pulse operation

Long pulse operation has allowed to gain insight on fuel retention, a crucial issue for ITER occurring on long time scales. We will review experimental results obtained using the following definitions (see Fig. 3 for illustration):

- Retained fraction during the pulse:

$F_{pulse} = N_{wall}/N_{inj}$ where N_{wall} is the wall inventory cumulated during the shot and N_{inj} the integrated particle injection.

- Short term retention, taking into account the recovery after the pulse:

$F_{short} = (N_{wall} - N_{rec})/N_{inj}$ where N_{rec} is the particle recovery after the shot.

- Long term retention, integrated over a campaign, taking into account the recovery between pulses, during the night (N_{night}), during cleaning procedures (N_{clean}), etc., ...:

$$F_{long} = \Sigma(N_{wall} - N_{rec} - N_{night} - N_{clean}...)/N_{inj}.$$

5.1. Experimental results on fuel retention

During the pulse, the retention rate Γ_{wall} exhibits common features in all devices [38]. Two phases can

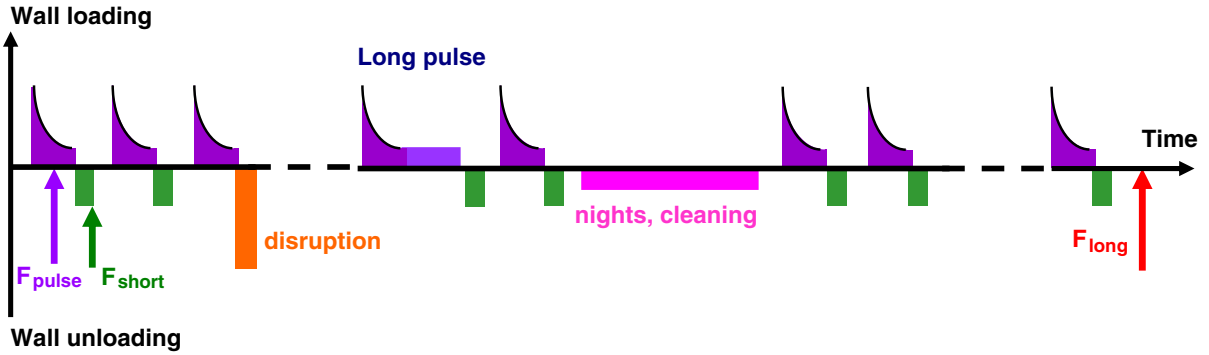

Fig. 3. Schematic view of the particle balance, showing the wall inventory build up during the shot (purple) and the recovery after shot (green). Recovery after a disruption (orange) or cleaning procedures (magenta) are also illustrated. Definitions of the retention fractions used in the text, such as F_{pulse} at the end of the pulse, F_{short} for the short term retention after the shot, and F_{long} for the long term retention integrated over a campaign, are indicated (For interpretation of the references to colour in this figure, the reader is referred to the web version of this article.).

be distinguished in time: a first phase where the retention rate is decreasing (from ~5 s in JET [39], ~10 s in JT60U [27] up to ~100 s in TS [40]), a second phase where it is constant (see the experimental retention rate shown on Fig. 8 for illustration). During the second phase, although it represents only a small fraction of the recycling flux (1–5%), F_{pulse} is always a significant fraction of the injected flux (50–80%). Fuelling methods (gas puff, pellets, supersonic molecular beam injection), active pumping, plasma density have very little impact on Γ_{wall} in the range explored so far in TS [40], while the LH power is seen to induce a linear increase of the retention rate [30]. The only exceptions where F_{pulse} is low are discharges with low fuelling rates, such as long L modes performed in JET [39], or saturated walls, such as repetitive long H modes performed in JT60U [27].

Concerning the dependance with fuelling rates, the same trend is found in AUG on short pulses [41], with net wall outgassing at low fuelling rate.

Concerning wall saturation, different behaviour is found depending if the machine is actively cooled or not. In TS (actively cooled), the retention rate has been found to be constant for more than 6 mn without sign of wall saturation. Shot to shot behaviour is identical, and no wall saturation has been found after 3 long discharges cumulating 15 mn of plasma operation. The cumulated inventory for the 3 discharges is much larger than what could be expected from saturation of the carbon PFCs surface [40].

In contrast, wall saturation is observed in non actively cooled devices, where the increase in PFC temperature during the shot can turn the wall from a net sink to a net source. This is observed in TRIAM-1M ultra long discharges, where the wall turns from sink to source after 35 mn during a 3 h discharge. This is correlated with the time evolution of the first wall temperature. When a cooled limiter is inserted in the discharge, limiting the PFC temperature increase, the wall remains a sink for a 5 h pulse in the same plasma conditions [16]. In JT60U, wall saturation does not occur in short pulses (<15 s), but appears progressively in repetitive long discharges [27,42][1]. The PFCs temperature offset is estimated to be of the order of 50–70 °C for the divertor plates (less for the first wall) from shot to shot, as the time between shots is not enough to let them cool down to their initial temperature. It is thought not to be significant enough to influence the maximum allowable concentration C_{Dmax} from shot to shot, and explain the progressive saturation observed. However, even moderate temperature increase has been shown to influence density control in TS (see Section 4). Interpretation remains difficult, as the accessible particle balance is only global, while different zones in the machine may play a role, such as zones in main interaction with the plasma, well conditioned by regular plasma operation, but reaching high temperatures (up to 1000 °C around the strike points at the end of the shot in the case of JT60U long H mode); 'cold' remote zones with moderate temperature increase but not properly conditioned ...

[1] The same phenomenon was observed for repetitive discharges in TS before the CIEL upgrade [43].

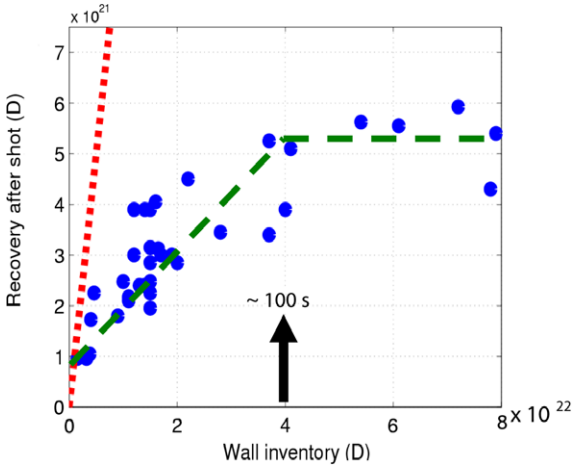

Fig. 4. Particle recovery after shot as a function of the wall inventory cumulated during the shot on TS [40]. The red dashed line corresponds to a recovery equal to the wall inventory, while the green line guides the eye to show that for shots longer than 100 s, the recovery is constant, independent of the cumulated inventory (For interpretation of the references to colour in this figure, the reader is referred to the web version of this article.).

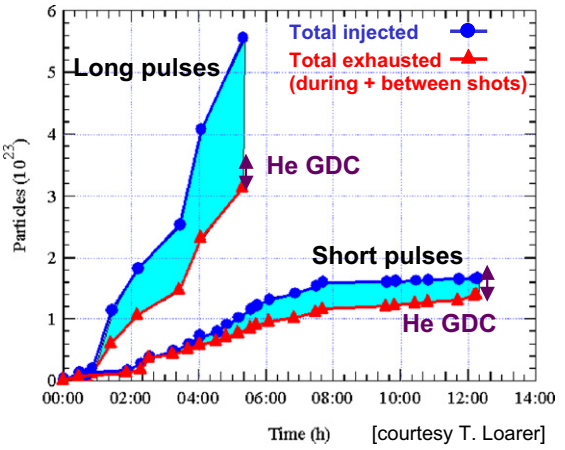

Fig. 5. Particle balance for 1 day of short and long pulses on TS [44]. The total quantities injected during the shot and exhausted during and between the shots are indicated, as well as the recovery by 1 night of He GDC for comparison.

The recovery after shot is always a small fraction of the wall inventory cumulated during the shot, as shown on Fig. 4, but it is however larger than the plasma content, showing that the wall does release particles. It is independent of the wall inventory for shots longer than 100 s on TS [40]. The same trend is found for AUG for the recovery by He GDC after the discharge [41]. Therefore, the short term retention fraction F_{short} is low for short pulses, while it is equivalent to F_{pulse} for long pulses, where the recovery after the shot becomes negligible compared to the wall inventory cumulated during the shot.

This difference is reflected when performing particle balance integrated over longer periods [38,44]. Fig. 5 shows particle balance performed for 1 shift of short pulses (~550 s of cumulated plasma time in 24 discharges) and 1 shift of long pulses (~1330 s of cumulated plasma time in 7 discharges) on TS. For short pulses, the inventory cumulated over the day can be compensated by a night of He GDC, yielding an overall balance close to zero. In contrast, long pulses lead to a significant inventory build up, much larger than the He GDC recovery. For most devices, the long term retention fraction coming from integrated particle balance ($F_{long} \sim 10$–20%) is larger than what is deduced from post mortem analysis of PFCs [45]. However, both these methods are subject to large error bars [2]: it is difficult to accurately estimate the recovery over long time periods for particle balance on the one hand [46,47], while post mortem analysis is often based on a restricted set of samples, and assumes toroidal/poloidal symmetry to reconstruct the global inventory on the other hand [48–51]. Extrapolation to ITER with $F_{long} = 10\%$, assuming a gas puff rate of 100 Pam^3 s^{-1} for 50–50% of D–T, yields an equivalent long term retention of 5 g of T per 400 s shot (which means in reality a higher value after the shot), therefore limiting the number of shots to 70 before reaching the safety limit of 350 g.

5.2. Interpretation of particle balance

To interpret this particle balance, several mechanisms of D retention in carbon have been invoked. They are quickly listed below, going in order of increasing concern for fuel retention issues.

- Adsorption in carbon porosity: transient mechanism (weak physical bond between D and C), saturates when open pores are filled.
- Implantation: permanent mechanism (strong chemical bond between C and D, no release unless heating, conditioning ...), saturates when C_{Dmax} is reached.

[2] T operation allows a better accuracy on the particle balance than for D. For T, $F_{long} = 35\%$ was found after the JET DTE1 campaign, although no long shots were performed. It was reduced to 10% after extensive cleaning with D and vessel venting [52].

- Bulk diffusion and trapping: permanent mechanism (chemical bond), does not saturate, but is thought to be negligible with diffusion coefficients found in literature.
- Codeposition: linked to the C source. Permanent mechanism (chemical bond), does not saturate.

The total retention rate will result from all of the above processes, with different features depending on which one is dominating. For instance, wall saturation will be observed if adsorption or implantation dominates, while it will not if bulk diffusion or codeposition do. The trapped fuel will be found mainly in plasma interaction zones if adsorption, implantation or bulk diffusion dominates, while it will be found rather in remote shadowed areas if codeposition does.

Adsorption could be a good candidate to explain the decreasing retention rate in phase 1. Indeed, it has been shown on TS that the recovery after shot is well correlated with the inventory cumulated during phase 1, suggesting that the responsible retention mechanism is transient [40]. Moreover, outgassing after the shot takes place on the same time scale than phase 1, which is consistent with the idea of filling/emptying the porosity reservoir. Analysis of deposited layers in TS have shown that they are significantly more porous than virgin CFC, and can adsorb up to 10^{22} D/g at low temperature/high pressure. The deposited layers found in TS (a few g) would therefore be sufficient to explain the inventory observed in phase 1 ($1–5\times10^{21}$ D), if the adsorption capacity is not significantly reduced in the tokamak environment (high T_{surf}, plasma pressure ...). This remains an open question.

Codeposition has been identified as the main concern for ITER, and is thought to be responsible for the retention observed in JET, in particular for the DTE1 tritium (T) campaign. Indeed, 3.7 g of T were still left in the vessel at the end of the campaign: 0.2 g were found when analysing divertor and main chamber tiles, another 0.5 g were found in 150 g of flakes, with high D/C ratio (D/C $\sim$ 1). To close the balance, the remaining 3 g are assumed to be in subdivertor flakes, which have been seen in the machine but could not be quantified ($\sim$1 kg needed when extrapolating from the 150 g analyzed) [52]. However, other machines have tried to estimate the codeposition rate Γ_{codep} by $\Gamma_C \times$ D/C, where Γ_C is the net carbon erosion/redeposition rate, and D/C the ratio determined from post mortem analysis[3]. The results found in TS and JT60U show that the net C source deduced from carbon balance is not sufficient to explain the experimental D retention rate with the measured D/C ratio (factor 20 for TS [40], 50-400 for JT60U [27]). Therefore, other retention mechanisms could be dominant.

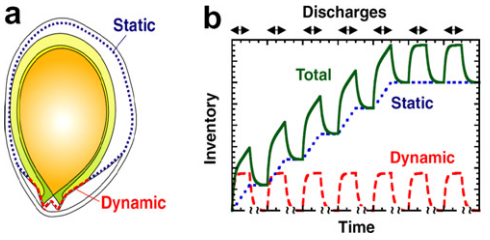

Fig. 6. Schematic explanation of wall behaviour in JT60U [42] with a dynamic implantation behaviour in the divertor region with strong temperature excursion, and a static implantation behaviour for the main chamber walls.

In JT60U, a tentative explanation of the wall behaviour is based on implantation [42]. Indeed, as in TS [54], saturation times going from less than 1 s up to 100s of seconds are evidenced, leading to zones immediately saturated (divertor plates), or within one pulse (baffles) or within several pulses (main chamber). The divertor region undergoes strong temperature excursions during the shot, and has therefore a dynamic behaviour as far as implantation is concerned, potentially going from particle sink to particle source. In contrast, the main chamber has a static behaviour, with a moderate temperature excursion. The wall behaviour (see Section 5.1) is then explained as illustrated in Fig. 6, with a superposition of the dynamic and static components. In short pulses, none of the above saturates. In long pulses, the dynamic component saturates within the pulse while it takes several pulses to saturate progressively the static component.

In TS, as the carbon source estimated from spectroscopy [55] as well as the D content found in deposited layers [48,49] seems insufficient to explain the experimental retention rate by codeposition only, other mechanisms have been investigated. Implantation of energetic cx neutrals has been estimated [54], and could play a role in the particle balance as they slowly saturate the main chamber

[3] Codeposition with Mo has also been reported in TRIAM [8,53].

walls, but can not explain identical shot to shot behaviour. Bulk diffusion has then been investigated. Indeed, it has been evidenced in laboratory experiments [56,57]. The exposure time to D bombardment is identified as a key parameter, as the same fluence delivered by cyclic and continuous exposure does not yield the same retained D fraction. In CFC, the retained D fraction is shown not to saturate but to increase as the square root of the fluence [57]. Bulk diffusion could also have been evidenced in tokamaks, as recent post mortem analysis of JT60U tiles have shown a long tail of D at low D/C close to the outer divertor strike point, in a zone dominated by net erosion [50] (several μm, well above the 10s of nm expected from implantation). Although it is difficult to bridge at present fundamental studies of hydrogen transport in carbon on the atomic scale, as presented in [58], with macroscopic results coming from tokamaks, they could show coherent features with the experimental observed behaviour, as shown in Fig. 7. Indeed, the first stage is gas permeation through open pores, which would correspond to the transient retention process seen in phase 1. Next stage is a molecular 'diffusion' (in fact successive dissociation/recombination of the molecule), which can lead to trapping at the edge of the crystallites (trap 2:90% of the available traps for non irradiated carbon), and then once these traps are saturated, to trapping in interstitial sites (trap 1:10% of the traps). The molecular diffusion would allow hydrogen to travel deep into the material, and would be the determining stage for the absorption rate. Trapping in trap 2 is pressure dependent, which could explain that long pulse with high particle fluxes, where significant pressure can be reached, could trigger this mechanism.

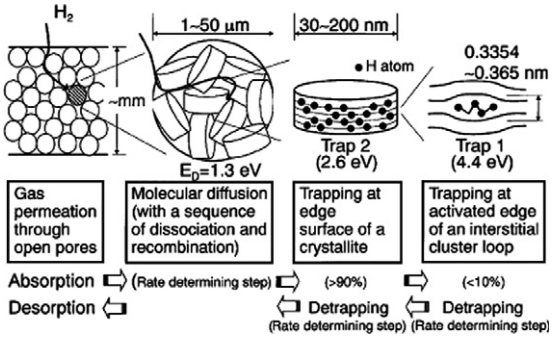

Fig. 7. Schematic illustration of hydrogen transport in carbon, taken from [58].

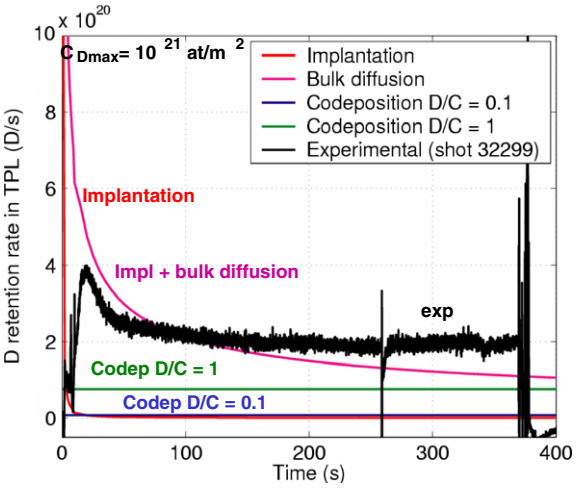

Fig. 8. Comparison of the experimental retention rate in TS with rough estimates of contribution from codeposition, implantation and bulk diffusion [48].

A preliminary application to the TS case is presented on Fig. 8, showing the experimental retention rate, together with the estimated codeposition rate, with D/C = 0.1 as measured, as well as D/C = 1 for comparison. As already stated, it seems difficult to account for the experimental rate by codeposition only. Contribution from implantation of the ion flux on the limiter, calculated as presented in [54] with saturation at $C_{\mathrm{Dmax}} = 10^{21}$ at/m^2 (corresponding to particles impacting with 300 eV energy [12]) is also shown: most of the limiter is immediately saturated, which can not explain the time behaviour of the retention rate. Finally, a simplistic model to estimate the contribution of the bulk diffusion is applied: implantation of the ion flux up to C_{Dmax} followed by an evolution of the retained fraction as the square root of the fluence as reported in [57]. As seen on Fig. 8, this could add a significant contribution to the retention rate. This result is however preliminary, and more work is needed to improve the model, with refined dependencies on impacting particles energy, temperature of the PFCs, and taking into account the cx neutrals as well as the ion flux as in [54].

5.3. Extrapolation to ITER

When trying to extrapolate these results (reminder: obtained in carbon dominated machines) to the T retention issue in ITER, the above processes are in order of growing concern:

- Adsorption: should concern a limited amount of T, which will be released after the shot (less than 0.5 g from a simple extrapolation on the carbon surface between present day devices and ITER. Indeed, assuming the release after shot in present devices (of the order of $1–5 \times 10^{21}$ D) is due to transient adsorption, and that it is only proportional to the carbon surface (roughly 10 times larger in ITER), one ends up with 0.12 g T for a 50–50% mix of D–T).
- Implantation: should again concern a limited amount of T (less than 5 g on a simple extrapolation for carbon surfaces again, up to 40 g if neutron irradiation/breeding is taken into account [59]). The main concern associated with the implanted fuel is linked to density control, as this process gives rise to a wall particle reservoir much larger than the plasma content, which can be partly released following a change in the PFCs surface temperature.
- Bulk diffusion: could play a role under the high particle flux and long pulse regime of ITER, but seems to behave like the square root of the fluence (better assessment is needed).
- Codeposition: is the major concern as it increases linearly with the fluence, and will be favoured by the low Te plasmas expected in ITER. Present simulations indicate less than 5 g/shot, but have large uncertainties [59].

6. Summary and prospects

With the ITER construction approaching, a growing awareness of the technological and physical challenges associated with steady state operation appeared, with emphasis starting to shift from peak to sustained performance in the experimental program of fusion devices. Significant progress has been achieved, with discharges longer than the required ITER pulse duration (400 s) and coupled energy larger than 1 GJ. However, the relevance of the present day experiments to the PWI issues for ITER is somehow restricted by the fact that there is no device combining the adequate plasma regime (semi detached at low Te), a realistic PFC material mix (all results reported in this paper are related to carbon PFCs only) and steady state PFC temperature ensured by active cooling (the only actively cooled device being the limiter tokamak TS).

The two main PWI limitations identified for long pulse operation are the following:

- localized heat loads associated with fast particle losses, leading to overheating and heavy impurity emission from unprotected metallic parts of the vessel;
- uncontrolled density rise, attributed to outgassing from heating PFCs rather than saturation by deuterium only, terminating the discharge in most experiments.

In all cases, improved PFCs cooling leads to better performances for long pulse operation. In particular, with active cooling of the whole vessel, including remote parts, as implemented in TS, density control has been demonstrated up to 6 min, the present limitation being the heating systems.

Fuel retention, a critical issue for ITER with long time scale, has been investigated. In most devices, the retention fraction during the shot is significant (50–80%), unless operating at low fuelling rate or with saturated walls. Wall saturation is observed in non actively cooled devices, where the wall can turn from a net particle sink to a net particle source as the PFC temperature increases, in contrast with actively cooled devices. The recovery after shot is shown to be independent of the wall inventory cumulated during the shot. Therefore, the overall balance is negligible when performing short pulses, while a significant wall inventory builds up when performing long pulses. Long term retention is around 10–20% in most devices, although they are not dominated by long pulse operation.

Different retention mechanisms have been identified. A transient adsorption of D through open pores of carbon could explain the particle recovery at the end of the shot. Codeposition of D with C is thought to be responsible for retention in JET, favoured by low Te plasmas allowing hydrocarbons transport, and cold remote areas in direct line of sight of the carbon erosion source, allowing deposited layers with high D/C ratio to grow. However, in other devices such as TS and JT60U, the carbon net erosion source does not seem to be sufficient to explain the experimental retention rate by codeposition only with the low D/C ratio measured in post mortem analysis ($D/C < 0.1$). In JT60U, where significant PFC temperature excursions occur during long pulses, implantation and outgassing are thought to be dominant in the overall particle balance, and could explain the wall global saturation behaviour. In TS, where the high Te plasmas do not favour chemical erosion (see

Table 2
Relevance of future long pulse experiments to ITER PWI issues

	SST-1 (2006)	KSTAR (2008)	EAST (2006)	JT60-SA (2013)	TS-CIMES (2008)	W7X (2012)
Configuration	Ax div	Ax div	Ax div	Ax div	lim	Isl div
PFC material	C	C	C	C (W)	C	C
Particle flux > 10^{22} D/m^2/s	no	yes	yes	yes	yes	yes
1 < Te < 10 eV (semi detach)	yes	yes	yes	yes	no	yes
Pulse > 1 mn	yes	yes	yes	yes	yes	yes
Power flux > 1 MW/m^2	no	yes	yes	yes	yes	yes
Active cooling	yes (bolted)	yes (bolted)	yes (bolted)	yes	yes	yes

Dark grey zones show significant deviation from ITER parameters.

Fig. 1 in [55]) and the stationary PFC temperatures ensured by active cooling prevent massive outgassing, bulk diffusion in the CFC has been invoked to explain the constant retention rate observed.

When extrapolating these results to the ITER T retention issue, adsorption and implantation should lead to a limited T inventory. However, the corresponding particle reservoir is much larger than the plasma content, and raises the issue of density controllability under saturated walls condition. Bulk diffusion could play a role, but seems to increase only with the square root of the fluence, while codeposition, increasing linearly with the fluence, remains the main concern. In both cases, detritiation is difficult: for bulk diffusion, T could penetrate deep into the material while for codeposition it could accumulate in remote areas such as gaps and subdivertor structures.

Prospects for steady state operation include the construction of a new generation of superconductive actively cooled divertor devices (see Table 2), partly filling the gap towards ITER. However, the main open issues related to mixed materials effects (including localized heat loads on Be and W, formation of Be/W alloys, properties of mixed redeposited layers, codeposition and bulk diffusion of T with Be ...), will not be addressed in these machines, still relying on carbon PFCs. Projects such as the ITER like Be/W/C wall in JET and the full W divertor in AUG, as well as experiments in PSI devices such as PISCES and MAGNUM, should allow to progress on these topics, although not in a fully steady state perspective.

Acknowledgements

The author acknowledges the help of many colleagues from the teams involved in long pulse operation, and in particular fruitful discussions with Dr Asakura, Ashikawa, Cordier, Ghendrih, Grosman, Loarer, Monier, Roth, Saoutic, Sakamoto, and Yang.

References

[1] B. Saoutic, Plasma Phys. Control. Fus. 44 (2002) B11.
[2] S. Ide et al., Nucl. Fus. (45) (2005) S48.
[3] T.C. Luce et al., Nucl. Fus. (45) (2005) S86.
[4] E. Joffrin, P. de Vries, R. Felton, et al., in: Proceedings of the 32nd EPS Conference on Plasma Phys., Tarragona, 2005.
[5] T. Mutoh, R. Kumazawa, T. Seki, et al., J. Plasma Fus. Res. 81 (4) (2005) 229.
[6] X. Gong and HT7 Team, J. Nucl. Mater., these Proceedings.
[7] B. Wan, J. Luo, J. Li, et al., Nucl. Fus. (45) (2005) S132.
[8] H. Zushi, K. Nakamura, K. Hanada, et al., Nucl. Fus. (45) (2005) S142.
[9] D.V. Houtte, G. Martin, A. Bécoulet, et al., Nucl. Fus. (44) (2004) L11.
[10] G. Federici, P. Andrew, P. Barabaschi, et al., J. Nucl. Mater. 313–316 (2003) 11.
[11] R. Doerner et al., J. Nucl. Mater., these Proceedings, doi:10.1016/j.jnucmat.2006.12.059.
[12] K.L. Wilson et al., in Atomic and Plasma Material interaction data for fusion, Supplement to Nuclear Fusion, IAEA, vol. 1 1991, p. 31.
[13] G. Federici et al., J. Nucl. Mater., these Proceedings, doi:10.1016/j.jnucmat.2007.01.260.
[14] M. Asif, X. Gao, J. Li, et al., Phys. Plasma 12 (2005).
[15] J.S. Hu, J.G. Li, X.D. Zhang, et al., Fus. Eng. Des. 73 (2005) 119.

[16] M. Sakamoto, M. Ogawa, K. Tagaki et al., in: Proceedings of the 32nd EPS conference on Plasma Phys., Tarragona, 2005, ECA (29C), P-5.005.
[17] R. Kumazawa, T. Mutoh, K. Saito, et al., Nucl. Fus. (46) (2006) S13.
[18] P. Garin et al., Fus. Eng. Des. 56&57 (2001) 117.
[19] H. Zushi, S. Itoh, K. Hanada, et al., Nucl. Fus. (43) (2003) 1600.
[20] M. Lipa, G. Martin, R. Mitteau, et al., Fus. Eng. Des. 66–68 (2003) 365.
[21] A. Ekehdal et al., J. Nucl. Mater., these Proceedings.
[22] F. Saint-Laurent, G. Martin, V. Basiuk, et al., J. Nucl. Mater. 337–339 (2005) 831.
[23] K. Saito et al., J. Nucl. Mater., these Proceedings, doi:10.1016/j.jnucmat.2007.01.269.
[24] M. Su, J. Nucl. Mater., these Proceedings, doi:10.1016/j.jnucmat.2007.01.236.
[25] C. Grisolia et al., J. Nucl. Mater. 266–269 (1999) 146.
[26] X. Gao, J. Li, Y. Yang, et al., J. Nucl. Mater. 337–339 (2005) 835.
[27] N. Asakura, Plasma Phys. Control. Fus. 46 (2004) B335.
[28] H. Takenaga, N. Asakura, S. Higahijima, et al., J. Nucl. Mater. 337–339 (2005) 802.
[29] K. Saito, R. Kumazawa, T. Mutoh, et al., J. Nucl. Mater. 337–339 (2005) 995.
[30] J. Bucalossi, C. Brosset, E. Dufour, et al., in: Proceedings of the 32nd EPS conference on Plasma Phys., Tarragona, (2005) ECA (29C), O-4.005.
[31] T. Nakano, J. Nucl. Mater., these Proceedings, doi:10.1016/j.jnucmat.2007.01.221.
[32] T. Nakano, S. Higashijima, H. Kubo, et al., J. Nucl. Mater. 313–316 (2003) 149.
[33] N. Ashikawa et al., J. Nucl. Mater., these Proceedings, doi:10.1016/j.jnucmat.2007.01.271.
[34] R. Guirlet, C. Brosset, J. Bucalossi, et al., in: Proceedings of the 32nd EPS conference on Plasma Phys., Tarragona, 2005.
[35] R. Guirlet, C. Brosset, B. Schunke, et al., in: Proceedings of 30th EPS Conference on Controlled Fusion and Plasma Physics, Saint Petersburg, 2003.
[36] P. Moreau et al., in: to appear in Proceedings of 24th Symposium on Fusion Technology, Warsaw, 2006.
[37] Y. Nakamura, Y. Takeiri, R. Kumazawa, et al., Nucl. Fus. (43) (2003) 219.
[38] T. Loarer, V. Philips, C. Brosset, et al., in: Proceedings of the 20th IAEA conference, Vilamoura, Portugal, 2004, IAEA CN 116/EX/5-22.
[39] T. Loarer, E. Tsitrone, C. Brosset, et al., in: Proceedings of the 30th EPS conference on Plasma Phys., St Petersburg, 2003.
[40] E. Tsitrone, C. Brosset, J. Bucalossi, et al., in: Proceedings of 20th IAEA Fusion Energy Conference, Vilamoura, 2004.
[41] V. Mertens, G. Haas, V. Rhode, et al., in: Proceedings of the 30th EPS conference on Plasma Phys., St Petersburg, 2003.
[42] H. Takenaga, T. Nakano, N. Asakura, et al., Nucl. Fus. (46) (2006) S39.
[43] C. Grisolia et al., J. Nucl. Mater. 196–198 (1992).
[44] B. Pegourie, C. Brosset, E. Delchambre, et al., Phys. Scr. T111 (2004) 23.
[45] T. Loarer, in: to appear in Proceedings of 21st IAEA Fusion Energy Conference, Chengdu, 2006.
[46] Y. Yang et al., in: Proceedings of the 32nd EPS conference on Plasma Phys., Tarragona, (2005), ECA (29C), P-4.002.
[47] J. Bucalossi et al., J. Nucl. Mater., these Proceedings, doi:10.1016/j.jnucmat.2007.01.071.
[48] C. Brosset, H. Khodja, J. Nucl. Mater. 337–339 (2005) 664.
[49] C. Brosset et al., J. Nucl. Mater., these Proceedings.
[50] T. Hayashi, K. Ochiai, K. Masaki, et al., J. Nucl. Mater. 349 (2006) 6.
[51] T. Hayashi et al., J. Nucl. Mater., these Proceedings, doi:10.1016/j.jnucmat.2007.01.112.
[52] N. Bekris, J.P. Coad, R.D. Penzhorn, et al., J. Nucl. Mater. 337–339 (2005) 659.
[53] M. Sakamoto, J. Nucl. Mater., these Proceedings, doi:10.1016/j.jnucmat.2007.01.055.
[54] E. Tsitrone, D. Reiter, T. Loarer, et al., J. Nucl. Mater. 337–339 (2005) 539.
[55] E. Dufour, C. Brosset, C. Lowry, et al., in: Proceedings of the 32nd EPS conference on Plasma Phys., Tarragona, 2005.
[56] B. Emmoth et al., Nucl. Fus. 30 (1990) 1140.
[57] J. Roth, J. Nucl. Mater., these Proceedings, doi:10.1016/j.jnucmat.2007.01.164.
[58] H. Atsumi, J. Nucl. Mater. 313–316 (2003) 543.
[59] G. Federici et al., IAEA workshop on in vessel T retention, Culham, 2003.